Temporal Small RNA Expression Profiling Under Drought Reveals a Potential Regulatory Role of snoRNAs in Drought Responses of Maize

Jun Zheng[*], Erliang Zeng[†, ‡], Yicong Du[*], Cheng He[§], Ying Hu[§1], Zhenzhen Jiao[*], Kai Wang[*], Wenxue Li[*], Maria Ludens[†], Junjie Fu[*], Haiyan Wang[**], Frank F. White[††], Guoying Wang[*#], Sanzhen Liu[§#]

[*] Institute of Crop Science, Chinese Academy of Agricultural Sciences, Beijing 100081, P.R.China

[†] Department of Biology, University of South Dakota, Vermillion, SD. 57069. U.S.A

[‡] Department of Computer Science, University of South Dakota, Vermillion, SD. 57069. U.S.A

[§] Department of Plant Pathology, Kansas State University, Manhattan, KS. 66506. U.S.A.

[**] Department of Statistics, Kansas State University, Manhattan, KS. 66506. U.S.A.

[††] Department of Plant Pathology, University of Florida, Gainesville, FL. 32611. U.S.A.

[1] Current address: Horticultural Sciences Department, University of Florida, Gainesville, FL 32611, USA

[#]To whom correspondence may be addressed:

Guoying Wang, Institute of Crop Sciences, Chinese Academy of Agricultural Sciences, Zhongguancun South Street 12, 100081, Beijing, China;

+86-10-8210-5862; wangguoying@caas.cn;

Sanzhen Liu, Department of Plant Pathology, Kansas State University, 4024 Throckmorton Center, Manhattan, Kansas, 66506;

+1-785-532-1379; liu3zhen@ksu.edu

Running title: Small RNA Regulation under Drought

Keywords: small RNA, drought, Zea mays, snoRNA, miRNA, epimark

Abstract

Small RNAs (sRNAs) are short noncoding RNAs that play roles in many biological processes, including drought responses in plants. However, how the expression of sRNAs dynamically changes with the gradual imposition of drought stress in plants is largely unknown. We generated time-series sRNA sequence data from maize seedlings under drought stress and under well-watered conditions at the same time points. Analyses of length, functional annotation, and abundance of 736,372 non-redundant sRNAs from both drought and well-watered data, as well as genome copy number and chromatin modifications at the corresponding genomic regions, revealed distinct patterns of abundance, genome organization, and chromatin modifications for different sRNA classes of sRNAs. The analysis identified 6,646 sRNAs whose regulation was altered in response to drought stress. Among drought-responsive sRNAs, 1,325 showed transient down-regulation by the seventh day, coinciding with visible symptoms of drought stress. The profiles revealed drought-responsive microRNAs, as well as other sRNAs that originated from ribosomal RNAs (rRNAs), splicing small nuclear RNAs, and small nucleolar RNAs (snoRNA). Expression profiles of their sRNA derivers indicated that snoRNAs might play a regulatory role through regulating stability of rRNAs and splicing small nuclear RNAs under drought condition.

Introduction

Physiological responses to drought in plants are complex and regulated through an interplay of a network of genetic components and chromatin structure. One component is comprised of drought-responsive small RNAs (sRNAs) (KHRAIWESH *et al.* 2012). sRNAs are short noncoding RNAs, predominately 20 to 24 nt in length, which function as sequence-specific regulators in a wide variety of biological processes, including DNA methylation, RNA degradation, translation regulation, and histone modification (KHRAIWESH *et al.* 2012; AXTELL 2013a). Plant sRNAs are typically categorized into two major groups, which are distinguished by the structure of the sRNA precursors. The first group consists of microRNAs (miRNAs), which are predominately 21 nt in length and processed from single-stranded precursor RNA, or pri-sRNA, are transcribed by RNA polymerase II (PolII) and contain a hairpin structure. The second group is comprised of small interfering RNAs (siRNAs) are derived from DICER/DICER-like processing of double-stranded RNAs (dsRNAs).

MiRNAs function in drought stress responses (COVARRUBIAS AND REYES 2010; SHUAI *et al.* 2013) and are, conceptually, categorized into three functional categories - homeostasis, detoxification, and growth regulation (ZHU 2002) and function largely through the destabilization of various transcription factors (RHOADES *et al.* 2002; DING *et al.* 2013; FERDOUS *et al.* 2015; ZHANG 2015). The function of miRNAs in the regulation of transcription factors places miRNAs at the hubs of gene regulatory networks for drought responses. Whereas miRNAs primarily act in the posttranscriptional regulation of gene expression, siRNAs regulate gene transcription through both guiding DNA

methylation by the pathway of RNA-directed DNA methylation (RdDM) and posttranscriptional destabilization of transcripts in a sequence-specific manner (ONODERA *et al.* 2005; WIERZBICKI *et al.* 2008). Small interfering RNAs can be further sub-grouped into heterochromatic siRNAs, secondary siRNAs, and natural antisense transcripts siRNAs (NAT-siRNA). Heterochromatic siRNAs, typically, are 23-24 nt in length and require RNA-dependent RNA polymerase (RDR) and RNA polymerase IV (PolIV) for biogenesis. Heterochromatic siRNAs were documented to be derived from transposable/repetitive elements located at heterochromatic regions of nuclear DNA (MEYERS *et al.* 2008; NOBUTA *et al.* 2008). Secondary siRNAs include trans-acting siRNAs (ta-siRNA), which are formed through cleavage of capped and polyadenylated siRNA transcripts by specific miRNAs, followed by conversion into dsRNAs by RDR (VAZQUEZ *et al.* 2010). NAT-siRNAs are derived from dsRNAs formed by annealing of natural sense and antisense transcripts from the same or separate nearly identical genomic regions (VAZQUEZ *et al.* 2010).

Small RNAs can also originate from ribosomal RNAs (rRNAs), transfer RNAs (tRNAs), small nucleolar RNAs (snoRNAs), and small nuclear RNAs associated with mRNA splicing (splicing snRNAs) and are respectively referred to as rsRNAs, tsRNAs, sno-sRNAs, and splicing sn-sRNAs hereafter (VAZQUEZ *et al.* 2010). The rsRNAs, tsRNAs, sno-sRNAs, and splicing sn-sRNAs play regulatory roles in cellular processes (MORRIS AND MATTICK 2014). In barley, tsRNAs and sno-sRNAs tended to be up-regulated and down-regulated, respectively, under drought conditions (HACKENBERG *et al.* 2015). In maize, miRNA biosynthesis and regulation under drought stress has been explored (LI *et*

al. 2013; LIU *et al.* 2014; WANG *et al.* 2014). However, the regulatory functions of sRNAs other than miRNAs are largely unknown.

To understand sRNA function and regulation in the drought response of maize, we sequenced sRNAs from maize seedlings over a period of 3 to 11 days after withholding water along with sRNAs from well-watered plants or drought treated plants that recovered after watering. The sRNAs were categorized with respect to length and functional classification, and the genomic organization of sRNAs was analyzed. An attempt was made to classify drought-responsive sRNAs using cluster and network analyses on the time-series expression patterns, providing clues of destabilization of ribosome RNA and splicing small nuclear RNAs under drought condition.

Materials and Methods

Plant materials and drought treatments

Seeds of the maize (*Zea mays*) inbred line B73 were surface-sterilized and germinated on the wet rolled brown paper towel at 28^{o}C for 48h, and eighteen germinated seeds were selected and transplanted in a plastic pot (17×12×10cm) filled with nutrient soil (1:1 peat moss and vermiculite). Three-day seedlings after germination were subjected to drought stress up to 10 days by withholding water (10 DAW), and the control plants were well watered. The plants were grown on the controlled conditions (27 ^{o}C day/23 ^{o}C night, 16 h photoperiod, from 6 am to 10 pm, 300µmol m^{-2} s^{-1} photons, 30-50% relative humidity). Treatment (drought stress) and the control pots were randomly laid in growth chamber. Eighteen seedlings were planted in a pot. For every harvest and sample time, five pots

were used for a drought treatment and other 5 pots were used as a control. At 10 DAW, drought treated seedling plants were divided into two groups: a group of seedlings kept under drought stress without watering and the other group of seedlings that were re-watered. In summary, 36 samples of soils and leaf tissues were collected: i) 32 samples resulting from 2 treatments (drought stress (DS) and well watered (WW)) x 8 days (from day 3 to day 10) x 2 biological replicates; ii) 4 samples resulting from 2 treatments (DS and WW at day 11th of plants previously subjected to 10 days of DS) x 2 biological replicates.

Measurement of soil SWC, leaf RWC, and leaf REC

Soil samples and leaf tissues for measuring SWC (soil water content), RWC (relative water content), and REC (Relative electrical conductivity) were daily collected at around 9:30 am. Five independent replicates were performed for the SWC measurement, and five biological replicates were performed for RWC and REC measurements. SWC, RWC, and REC were carried out according to the previously described method (ZHENG *et al.* 2010). Briefly, the soil SWC was the percentage of the weight loss of soils after drying. The RWC of the fresh leaves was calculated using the formula of (FW-DW)/(TW-DW) x100%, where FW is the weight of fresh leaves, TW is the leaf weight after saturated in water for 8 h, and DW is the leaf dry weight. REC was calculated using Ec1/Ec2 x 100%, where Ec1 is electrical conductivity of fresh leaves after saturated in water for 3 h and Ec2 is electrical conductivity of the same leaf samples after boiled in a water bath.

sRNA sequencing experiment

The above ground tissues of five seedlings of each treatment at each day were collected at approximately 10 am each day and immediately frozen in liquid nitrogen. Total RNA was isolated from harvested samples using TRIzol reagent (Invitrogen). A standard Illumina small RNA library preparation kit was used to prepare small RNA sequencing libraries from total RNAs. Briefly, a total of 2 μg sRNAs in the size range of 15 to 30 nucleotides were purified and ligated to 3' adaptor, and isolated by 15% denaturing polyacrylamide gel electrophoresis gels to eliminate un-ligated 3' adaptors. The products were ligated to 5' adaptor and then were used to conduct reverse transcription PCR. The final PCR product was isolated by 3.5% agarose gel electrophoresis and served as a small RNA library for the sequencing. The libraries were quantified and sequenced at HiSeq2000 analyzer to produce single-end 50 bp reads. Two biological replicates were employed in the sRNA sequencing experiment.

sRNA data process

Trimmomatic (version 0.32) was used to trim the adaptor sequence of sRNA reads. The parameters used for the trimming is: "ILLUMINACLIP:adaptor_seq:2:30:7: LEADING:3 TRAILING:3 SLIDINGWINDOW:4:13 MINLEN:16". The adaptor sequence (adaptor_seq) includes a sequence of "CTGTAGGCACCATCAATCAGATCGGAAGAGCACACGTCTGAACTCCAGTCAC". These parameters were used to perform both adaptor and quality trimming. Although quality trimming could shorten actual sRNAs, the percentage of reads subjected to quality trimming is only ~0.3%. Therefore, quality trimming was applied to remove the

low quality of nucleotides at the marginal compromise of changing sRNA lengths. At least 16 nt in size was required for clean reads.

A non-redundant sRNA (NR-sRNA) set was obtained by pooling sRNAs from all the samples and remove the redundancy. To remove most sRNA sequences that carry sequence errors, only sRNAs that were shown in at least two different samples and at least twice in each sample were included in the unique sRNA set. After determining read counts of each sRNA from all 36 samples, a further reduction was performed to only keep sRNAs with at least 72 reads summed from all the samples, equivalent to 0.08 reads per million of total reads, resulting in a NR-sRNA set.

Functional annotation of sRNAs

The small RNA annotation database was downloaded from Rfam 11.0 (BURGE *et al.* 2013). sRNAs generated from this experiment were aligned to Rfam 11.0 database using Blastn (BLAST 2.2.29+) with the following parameters (-evalue 1e-1 –word_size 10 –perc_identity 0.89 –strand plus –best_hit_overhang 0.2 –best_hit_score_edge 0.1 –outfmt 6 –max_target_seqs 10). The sRNAs was functionally annotated only if they were unambiguously hit an Rfam family.

Alignment to the reference genome to determine copy number of sRNA regions

Each sRNA was aligned to the B73 reference genome (RefGen2 and 4) using bwa (version 0.7.5a-r405) (LI AND DURBIN 2010). The command parameters were “bwa aln –l 18 –k 0 –t 48 –R 22500” followed by “bwa samse –n 22500”. The alignments were then

parsed with the stringent criteria: perfect match with at least 18 bp matching length. These alignment and parsing criteria allow the maximal 22,500 perfect hits.

K-mer analysis using sequencing data to determine copy number of sRNA genomic regions

B73 whole genome shotgun Illumina sequencing data were downloaded from Genbank (SRR444422). Trimmomatic (version 0.32) was used for the adaptor and quality trimming with the same parameters to those used in the sRNA data trimming. The adaptor sequences used for the adaptor trimming are (TACACTCTTTCCCTACACGACGCTCTTCCGATCT and GTGACTGGAGTTCAGACGTGTGCTCTTCCGATCT). The clean data were subjected to error correction using the error correction module (ErrorCorrectReads.pl) in ALLPATHS-LG (BUTLER *et al.* 2008) with the parameters of "PHRED_ENCODING=33 PLOIDY=1". We then used the corrected sequencing data to perform k-mer counting using the count function in JELLYFISH (MARCAIS AND KINGSFORD 2011) with the parameters of "-m k-mer –L 2 –s 100M –C", where the k-mer was from 18 to 30 nt. Once the read depth of each k-mer from 18 to 30 nt was counted, the read depth of a corresponding sRNA can be determined. The highest density of k-mer counts was located at 26.96 for a set of known single copy k-mers determined by reference genome alignments, indicating approximately 26.96x sequencing depth was obtained. This number was used as the base of read depths of a single copy to adjust counts of each k-mer to roughly represent its genome copy number.

207 **Determination of mean levels of various histone modifications**

208 ChIP-Seq data of H3K27me3, H3K36me3, H3K4me3, and H3K9ac (WANG *et al.* 2009),
209 and H3K9me2 (WEST *et al.* 2014) of 14-day B73 seedlings were downloaded from
210 Genbank. To match sequencing data to sRNA sequences, ChIP-Seq data were subjected
211 to k-mer counts at different k-mer lengths from 18 to 26 nt using JELLYFISH (MARCAIS
212 AND KINGSFORD 2011). Through k-mer counts, read counts from ChIP-Seq data of each
213 sRNA sequence was determined. Using sequencing read counts of whole genome
214 sequencing (WGS) data of sRNA sequences as the control, the histone modification
215 signal of each sRNA, represented by ChIP read count divided by WGS read count of an
216 sRNA, was calculated. Due to the lack of biological replication and the limited
217 sequencing depth of ChIP-Seq data, we did not attempt to assess the histone modification
218 level of each sRNA. Instead, mean of histone modification levels of all sRNAs in a
219 certain functional group (e.g., miRNA, rsRNA) were determined and used as the
220 modification level of that sRNA group for the comparison between functional groups.
221 Comparisons were only performed within the same length of sRNAs.
222
223 To enable the comparison of histone modification levels among different lengths of
224 sRNAs, all lengths of sRNAs from 18 to 26 nt were converted to 18 nucleotide fragments
225 and the average signal of five epimarks were determined separately. As a control, 18 nt of
226 different genic regions, promoters, first exons, internal exons, introns, and last exons,
227 were sampled and the average histone modification levels of five epimarks of each genic
228 region were calculated.
229

Identification of drought-responsive sRNAs

A generalized linear model was fitted for each sRNA to identify drought responsive sRNAs. The response variable in the model is the read count of an sRNA, which were assumed to follow negative binomial distribution. The model contains two factors, DAW (day) and treatment, and their interactions. The DAW has eight factor levels (from 3 to 10) and the treatment has two factor levels (DS and WW). A deviance test of no interaction effect between DAW and treatment was conducted for each sRNA. The generalized linear model fit and test, assuming a negative binomial distribution for read counts, were implemented in DESeq2 (LOVE *et al.* 2014). sRNAs having at least five reads on average per sample were used for the statistical test, resulting in a p-value from each sRNA. A false discovery rate (FDR) approach was applied to account for multiple comparisons (BENJAMINI AND HOCHBERG 1995). Significant sRNAs were declared using the 5% FDR as the cutoff. The script was deposited at GitHub (https://github.com/liu3zhenlab/sRNAs_drought).

Clustering of drought-responsive sRNAs

Drought responsive sRNAs were subjected to clustering analysis using mclust (FRALEY AND RAFTERY 2007). For each drought-responsive sRNA, the Log2 of the ratio of the mean of DS expression (the normalized value) to the mean of WW expression (the normalized value) at a certain DAW (day) was determined, which represents the Log2 of the fold change in expression between DS and WW. Log2 ratio values were then used for the clustering analysis. The script was deposited at GitHub (https://github.com/liu3zhenlab/sRNAs_drought).

253

254 **Identification of significantly differentially expressed sRNAs between DS and water**
255 **recovery**

256 To test the null hypothesis that no difference in sRNA expression between two groups at
257 11 DAW, DR and water recovery (DWR), generalized linear model for the read count of
258 each sRNA implemented in the DESeq2 package (version 1.4.5) was used (LOVE *et al.*
259 2014). A false discovery rate (FDR) approach was used to account for multiple tests
260 (BENJAMINI AND HOCHBERG 1995). The FDR 5% was used as the cutoff for declaration
261 of differential expression.

262

263 **Enrichment analysis**

264 The enrichment analyses were performed for determining if a certain type of category,
265 such as a member of sRNA functional families, is over-represented in a selected group of
266 sRNAs. To account for the biases read depth that influences the selection of members in a
267 certain group, the resampling method in the GOSeq enrichment test (YOUNG *et al.* 2010)
268 with the bias factor of read depth, total reads across all the samples of a certain sRNA,
269 was applied to enrichment analyses.

270

271 **Analysis of sRNA co-expression network**

272 Drought-responsive sRNAs (FDR < 1%) were used to build co-expression sRNA
273 network using Bioconductor package WGCNA (v1.51) (LANGFELDER AND HORVATH
274 2008). WW sRNA network was built using sRNA expression profiles in WW samples,

and DS sRNA network was constructed using sRNA expression profiles in DS samples. The package WGCNA uses an appropriate soft-thresholding power to construct a weighted gene network. Modules of highly correlated sRNAs were identified using topological overlap measure (TOM) implemented in WGCNA. Module preservation analysis was also performed using WGCNA, with DS network as a test and WW network as a reference, and vice versa. An R script for network analysis has been deposited at GitHub (https://github.com/liu3zhenlab/sRNAs_drought).

Identification of miRNAs

The database of mature miRNAs was downloaded from miRBase v22 (ftp://mirbase.org/pub/mirbase). In total, 325 mature B73 maize miRNAs from 174 miRNA genes were extracted. Any sRNAs discovered in this study identical to these mature miRNAs were annotated as known miRNAs.

ShortStack (v3.8.5) was used to *de novo* identify a set of miRNAs with the parameters (--dicermin 18 --dicermax 30 --mismatches 0 --mincov 0.5rpm), and using B73Ref4 (version 4) as the reference genome (AXTELL 2013b). ShortStack identified novel miRNA loci that did not overlap with any known miRNA genes. Any mature miRNAs from novel miRNA loci were referred to as novel miRNAs. Some mature miRNAs from ShortStack are not known miRNAs but from known miRNA genes. Combining both known mature miRNAs and all newly discovered mature miRNAs by ShortStack using our massive sRNA datasets, we updated the miRNA set, referred to as B73miRBase22plus.

298

299 **Identification of IsomiRs**

300 IsomiRs are variants of the reference mature miRNAs (MORIN *et al.* 2008). An isomiR in
301 this study is a small RNA perfectly matching a pri-miRNA but with a different sequence
302 from mature miRNAs in the B73miRBase22plus. Only 20-22 nt sRNAs identical to the
303 plus-stranded sequence of a region of pri-miRNAs were referred to as isomiRs.

304

305 **Identification of ta-siRNAs**

306 sRNAs matching ta-siRNA downloaded from tasiRNAdb
307 (http://bioinfo.jit.edu.cn/tasiRNADatabase/) were defined as known tasiRNA. Also
308 sequences of maize trans-acting siRNA 3 (TAS3) were retrieved from Dotto et al.
309 (DOTTO *et al.* 2014).

310

311 **Degradome analysis of drought-responsive miRNAs**

312 Degradome raw reads were obtained from a previous maize miRNA study (LIU *et al.*
313 2014). After removing adaptor sequences and low-quality sequencing reads, clean reads
314 were used to identify cleavage sites based on B73 cDNA sequences (5b+). CleaveLand
315 4.0 was implemented for degradome analysis with the default parameters (ADDO-QUAYE
316 *et al.* 2009), which provides evidence for gene targeting by miRNAs or isomiRs.

317

318 **Prediction of miRNA targeted genes and GO enrichment analysis of targeted genes**

319 psRNATarget (http://plantgrn.noble.org/psRNATarget/) was used to predict miRNA
320 target genes (DAI AND ZHAO 2011) . Gene targets of miRNAs were predicted based on

B73 AGPv3.22 annotated transcript sequences with the expectation value no more than 1.5. Gene ontology (GO) enrichment of predicted miRNA-targeting genes was analyzed with AgriGO (TIAN *et al.* 2017).

Transposable element analysis of 24 nt genomic loci

sRNA genomic clusters, from the ShortStack result, predominant by 24-nt sRNAs were referred to as 24-nt genomic loci. RepearMasker (open-4.0.5) was used to identify sequences matching transposable elements with the maize transposon database. As a control, the "shuffle" module in the bedtools was employed to randomly select intervals simulating the number and sizes of genomic intervals of 24-nt loci.

Data Availability

The datasets supporting the conclusions of this article are included within the article and its supplemental materials. Supplemental files available at FigShare. All sRNA sequencing raw data were deposited at Sequence Read Archive (SRA) (accession number: SRP081275).

Results

Physiological changes of seedlings under drought conditions

Maize seedlings were subjected to drought over a period of nine days (**Figure 1A**). Three-day-old B73 seedlings after germination were subjected to two treatments, drought stress (DS) and well-watered (WW). Above ground tissues (referred to here as leaves) were collected at 3 to10 Days After Withholding water (DAW) or with watering with two

biological replicates at each day. At 10 DAW, some seedlings from the DS treatment group were subjected to two treatments: continuously withholding water (DS) and re-watering, both of which were sampled at the 11th day. Two biological replicates were collected, resulting in two additional DS samples on day 11 and two re-watering samples at one day after addition of water at day 10. A total of 36 plant samples were processed. Compared to WW seedlings, DS-treated seedlings showed severe stressed phenotype by 8 DAW. Soil water content (SWC) decreased in the DS treatment from ~60% to 20% in the same period (**Figure 1B**). Leaf relative water content (RWC) of DS seedlings also decreased upon the drought treatment, at a low declining rate from 3 to 7 DAW and a high rate after 7 DAW (**Figure 1C**). Leaf relative electrical conductivity (REC), which is a measure of cellular damage, exhibited strongest response to drought between 8 and 9 DAW (**Figure 1D**), indicating that leaf cells began to experience damage after 8 DAW under drought conditions. The DS-treated seedlings showed visible stressed phenotypes after 10 DAW. When re-watered at 10 DAW, the DS-treated plant seedlings were visibly recovered at 11 DAW.

Characterization of sRNAs

The 36 RNA samples were extracted for sRNA sequencing, resulting in more than 886.6 millions of 50 bp single-end reads, from 20.5 to 34.2 millions reads per sample. On average, 97.5% of reads were retained after adaptor and quality trimming of each sample (**Table S1**). The majority of sRNAs were between 18 and 26 nucleotides (nt). The 24-nt sRNA length class was the largest, followed by the 21 nt and 22 nt sRNA classes (**Figure**

366 **2A**). The same pattern of length distribution was observed across all the samples,
367 indicating that the drought treatment did not alter the global pattern of sRNA lengths.
368
369 All sRNA reads from the 36 samples were merged, and sRNAs with at least 72 reads
370 were retained. Removing redundant reads with the same sequence for each sRNA
371 resulted in a non-redundant sRNA (NR-sRNAs) set of unique 736,372 sRNAs (134,283
372 NR-sRNAs used in the later time-series statistical analysis were listed in **Table S2** and
373 **Table S3**. The NR-sRNAs set was annotated using the Rfam database (Rfam11.0). 12.4%
374 (91,473) of the NR-sRNAs could be unambiguously annotated with regard to function
375 (see Methods). Among the Rfam-annotated subset of sRNAs, rsRNAs, tsRNAs, and
376 miRNAs are the most abundant, comprising of 40%, 27%, and 7%, respectively (**Figure**
377 **2B**). The rsRNA and tsRNAs represented nearly 70% of all annotated NR-sRNAs, while
378 miRNAs distributed in a slightly narrower length range of 18 to 24 nt and a peak length
379 at 21 nt (**Figure 2C**). Of 21 nt NR-sRNAs, 22% are miRNAs from approximately 65% of
380 the total 21-nt sRNA reads (redundant sRNAs), indicating that some 21 nt miRNAs were
381 highly expressed (**Figure 2C, 2D**). Indeed, the single sRNA showing the highest
382 abundance is a miR159, with 14.8 million reads.
383
384 **Genome organization of NR-sRNAs in B73**
385 The copy number of individual NR-sRNAs in the B73 genome was estimated by both
386 mapping reads to the B73 reference genome (reference-based) and analyzing sequences
387 present in whole-genome-shotgun sequence reads (WGS-based) (see Methods). A small
388 number of NR-sRNAs, 20,452, were excluded based on alignment to either chloroplast or

mitochondria DNA. Among the remaining NR-sRNAs (N=705,920), perfect matches for 93.2% of the NR-sRNAs were identified in either the B73 reference genome or the B73 WGS data. The absence of perfect matches for 6.8% of the NR-sRNAs was attributed to incomplete B73 genome assembly, contamination, sequencing errors, and/or RNA editing (LIANG AND LANDWEBER 2007; SCHNABLE *et al.* 2009). The estimations of copy number from the two approaches were largely consistent (**Figure S1**). Both estimations indicated that most NR-sRNAs are from low-copy genomic loci (1-2 copies) except for NR-sRNAs from rRNA and tRNA (**Figure S2**). NR-sRNAs of differing lengths exhibit varying mixtures of low- and high-copy loci (**Figure S3**). The 24 nt sRNAs are mostly single copy in the genome, while a high proportion of 21-23 nt sRNAs are derived from either low-copy or very-high-copy genomic loci. Outside of the 21-24 sRNA range, NR-RNAs from highly repetitive genomic regions are dominant (**Figure S3**).

A linear association between expression level and genomic copy number of sRNAs was not observed (**Figure S4**). Genomic single-copy NR-sRNAs can be highly expressed. For example, the single copy miR168 locus was expressed at a high level (138,292 reads). Conversely, the expression of most genomic high-copy NR-sRNAs was low. Some high-copy NR-sRNAs were highly expressed, such as rsRNAs. Analysis of sRNA expression profiles based on functional classes also showed that high proportions of splicing sn-sRNAs and sno-sRNAs exhibit low expression, while many rsRNAs were expressed at a high level (**Figure 2E**). The 23 and 24 nt sRNAs, regardless of functional classes, were mostly expressed at a low level, while 20-22 nt sRNAs tended to be expressed at

411 relatively higher levels (**Figure 2F**). Compared to 21-24 nt sRNAs as a whole, a higher
412 proportion of 20 nt sRNAs were highly expressed (**Figure 2F**).
413
414 **Distinct histone modifications at genomic regions of different classes of sRNAs**
415 Histone modification status at genomic regions of sRNAs was collected from genome-
416 scale data repositories for B73 seedlings, including multiple histone modifications:
417 H3K27me3, H3K36me3, H3K4me3, H3K9ac, and H3K9me2. The lack of biological
418 replication and low depth of most chromatin modification data limited assessment of
419 histone modification levels for each sRNA locus. Therefore, the mean of histone
420 modification levels of genomic regions in each functional sRNA class was used to
421 represent the overall genomic modification level of each sRNA functional class. To avoid
422 systematic biases, we compared histone modifications among different functional classes
423 at the same sRNA length (**Figure 3**, **Figures S5-S8** and **Table S4**). Average histone
424 modification levels on different functional classes showed that both miRNAs and sno-
425 sRNAs in size of 20, 21, and 23 nt were predominately found in open chromatin regions,
426 which were characterized by high modification levels of two hallmarks of open
427 chromatin regions, H3K4me3 and H3K9ac. The H3K4me3 signal at sno-sRNA genomic
428 regions was much higher than those of genomic regions of any other functional sRNA
429 classes across all lengths from 20 to 24 nt. Genomic regions of 21 nt miRNAs and sno-
430 sRNAs, overall, had moderate levels of a silent chromatin mark H3K9me2, and genomic
431 regions of 20 and 23 nt miRNAs and sno-sRNAs exhibited low levels of H3K9me2
432 signals. H3K9me2 is associated with CHG (where H is A, T, or C) cytosine methylation
433 (STROUD *et al.* 2013; WEST *et al.* 2014), indicating that genomic regions producing

miRNAs and sno-sRNAs, on average, exhibited low CHG cytosine methylation. At the lengths of 20, 21, 23 nt, miRNA genomic regions had high levels of H3K27me3, a repressive chromatin mark associated with gene silence (GAN *et al.* 2015), and relatively low H3K36me3 levels that are generally positively associated with transcriptional activity but also were found to be enriched at heterochromatin regions (CHANTALAT *et al.* 2011). The sno-sRNA genomic regions, relative to miRNA genomic regions, exhibited the opposite modification pattern with low H3K27me3 levels and high H3K36me3 levels. Genomic regions of rsRNAs, splicing sn-sRNAs, and tsRNAs had similar histone modification patterns, namely, low levels of H3K27me3, H3K36me3, H3K4me3 and H3K9ac and a high level of H3K9me2 across all lengths from 20 to 24 nt.

Through converting all lengths of sRNAs to the same 18 nt length, average signals of histone modifications were compared among genomic regions producing different lengths of sRNAs. As the control, 18 nt DNA fragments were also randomly sampled from different genic regions, and their mean signals of histone modifications were determined. The results showed that, except for H3K36me3, all epimarks shared a similar trend that the modification signals were at a relatively high level for genomic regions of small lengths of sRNAs and gradually decrease until at 24 or 22 nt, followed by elevated modification signals (**Figure S9**). For open chromatin marks H3K4me3 and H3K9ac, on average sRNAs exhibited lower levels relative to promoters and first exons but similar levels to internal exons, introns and last exons. Our result showed that H3K9me2 was generally at much higher levels on sRNA genomic regions relative to genic regions, of which 24 nt sRNAs whose genomic regions had the closest H3K9me2 signal to genic

457 regions. That indicated that the CHG cytosine DNA methylation at genomic regions of 24
458 nt sRNAs is generally low.
459
460 **Identification of drought-responsive sRNAs**
461 A statistical test was performed to detect any interaction between drought stressed and
462 well-watered plants for each sRNA that had a minimum five sRNA reads per sample over
463 the 3 to 10 DAW period. The analysis revealed that 6,646 of the total 134,283 sRNAs
464 exhibited interactions between the DAW and the treatments at the 5% false discovery rate
465 (FDR) level (**Table S3**). Interacting sRNAs showing different responses under DS and
466 WW conditions at certain DAWs were scored as drought-responsive sRNAs. The
467 rsRNAs and 22 nt sRNAs are the two predominant groups in the drought-responsive
468 sRNA set (**Figure S10**). The DS-to-WW ratios of sRNA expression were further
469 subjected to cluster analysis using mclust (FRALEY AND RAFTERY 2007), resulting in 10
470 clusters. The sRNAs of clusters 3, 4, 5, 7, and 9 exhibited a pattern of up-regulation
471 under drought stress (**Figure 4A-F**), while sRNAs of clusters 1 and 8 showed a pattern
472 for down-regulation (**Figure 4G-I**). More than five times up-regulated sRNAs (N=4,373)
473 were detected than down-regulated sRNAs (N=816) under drought stress (**Figure 4**). The
474 enrichment analyses indicate that rsRNAs and splicing sn-sRNAs were over-represented
475 in up-regulated sRNAs, while miRNAs and sno-sRNAs were over-represented in down-
476 regulated sRNAs. Additionally, sRNAs of clusters 2 and 6 exhibited transiently down-
477 regulation on drought (transiently down-regulation group, N=1,325), which were down-
478 regulated at around 7 DAW when drought stress became intense, followed by a gradual

recovery of expression (**Figure 4J-L**). The enrichment analysis indicates that miRNAs and sno-sRNAs are significantly over-represented in transiently down-regulated sRNAs.

A comparison of sRNA expression was performed between two additional seedling groups at 11 DAW, DS and drought water recovery (DWR), which was re-watered on 10 DAW. Using the 5% FDR cutoff, 7,140 sRNAs were differentially expressed between two groups, of which 2,264 and 4,876 sRNAs were up-regulated and down-regulated in DWR relative to DS, respectively, and 486 were identified as drought-responsive sRNAs in the time-series analysis (**Table S3, S5**). The 473 sRNAs (out of 486) were classified into three groups in the time-series analysis: Down-regulated (N=43), up-regulated (N=426), and transiently down-regulated (N=4). All 43 sRNAs from the down-regulated group were up-regulated after DWR. Of 426 sRNAs in the up-regulated group, 76.3% (325/426) sRNAs showed decreased expression in DWR, while 23.7% (101/426) were continuously up-regulated even with water recovery. All four sRNAs in the transiently down-regulated response group were up-regulated after re-watering. Overall, the expression levels of most drought-responsive sRNAs were restored towards levels of well-watered plants upon re-watering.

Characteristics of co-expression networks of drought-responsive sRNAs

DS and WW weighted co-expression networks were constructed using WGCNA (LANGFELDER AND HORVATH 2008). Both networks consist of a subset of drought-responsive sRNAs with the FDR cutoff of less than 1% from the drought response statistical test. The DS and WW networks were built using normalized sRNA counts of

DS and WW samples, respectively (**Figure 5A, 5B, Table S3**). Network statistics indicate intrinsic differences between the two networks (**Table S6**). Although the DS and WW networks share similar network clustering coefficients, network centralizations, and network densities, the DS network (**Figure 5B**) has the smaller network diameter and lower heterogeneity, indicating expression of these drought-responsive sRNAs were more correlated upon drought stress or tended to be co-expressed in response to drought stress.

Modularity analysis in the DS network and the WW network further revealed that the two networks have different topology structures. Modularity analysis included two steps: module identification and module preservation analysis. Modules are sub-networks, consisting of co-expressed sRNAs. The sRNAs in the same module are similar in expression to some degree, thereby are likely associated each other. Module preservation analysis is used to determine if the topology of a network module identified in one network changes in the other network. For example, a module is considered preserved in the DS network, if its topology, based on preservation statistics, largely remains in the WW network. The module preservation analysis identified a preserved module (blue module) in the DS network compared to the WW networks (**Figure 5C**) and a preserved module (blue module) in the WW network in comparison to the DS networks (**Figure 5D**). Most sRNAs (N=546) in two blue modules overlapped, of which more than 95% are from the transiently down-regulated group (**Table S3**). The result indicated transiently down-regulated sRNAs tended to be co-regulated in both drought and well-watered conditions. On the other hand, these sRNAs exhibited a transient down-regulation to drought, which might serve as the signal to induce downstream drought responses. Of

546 overlapping sRNAs, 343 and 178 are 22 nt and 24 nt sRNA, respectively, and a few were functional annotated with the Rfam database (6 miRNAs and 9 sno-sRNAs). The module preservation analysis also revealed differences between modules in the DS and WW networks. The yellow module in the DS network is the least preserved module, indicating sRNAs of the module were perturbed in response to drought stress (**Figure 5C**). Indeed, the yellow module consists of 38 sRNAs that were down-regulated upon drought stress. In the WW network, the green module is the least preserved one, and most sRNAs were up-regulated upon drought.

Identification of drought-responsive miRNAs and the corresponding targeted genes

sRNA homologous to Rfam miRNAs were referred to as miRNAs hereinbefore. We refined the miRNA set based on the dedicated miRNA database, miRBase (KOZOMARA AND GRIFFITHS-JONES 2014), and *de novo* discovery of miRNAs from our massive datasets. We employed the ShortStack pipeline (AXTELL 2013b) and identified 53 miRNA loci of which 47 loci are known maize miRNA genes in miRBase (v22) containing 174 miRNA genes. We found 59 new mature miRNAs from, including 47 mature miRNAs from known miRNA loci but with different sequences of mature miRNAs, as well as 12 mature miRNAs from 6 novel miRNA loci. Requiring at least an 18 nt match with at least 90% identity, homologs of miRNAs from three novel miRNA loci (Cluster_23765, Cluster_27697, and Cluster_45700) were identified in MIR1878, MIR156c, and MIR166d, respectively. We combined both known and newly discovered mature miRNAs to create a new miRNA set referred to as B73miRBase22plus (**Table S7**) that contains 180 miRNA genes producing 392 mature miRNAs, of which 244 are

548 non-redundant miRNAs (**Table S8**). We also identified 608 isomiRs that are in length of
549 20-22 nt and identical to a region of a pri-miRNA sequence, but different from 392
550 mature miRNAs in sequence (**Table S9**).
551
552 Some miRNAs were highly expressed. The top eight most highly expressed miRNAs
553 belong to six families: miR159, miR168, miR396, miR156, miR169, and miR167 (**Table**
554 **S8**). Although highly expressed miRNAs, statistically, are most likely to be detected,
555 none of the top 25 miRNAs showed evidence of regulation under drought condition,
556 indicating that expression levels of most highly expressed miRNAs were kept at
557 relatively stable levels under drought stress. In total, 21/244 miRNAs and 18/608 isomiRs
558 showed significantly drought responses (**Table 1**). Most drought-responsive miRNAs
559 (N=13) were down-regulated by drought treatment, while four were up-regulated. The
560 remaining four were not categorized to any of the three major cluster groups. The 21
561 drought-responsive miRNAs belong to 13 families, including miR1432, miR156,
562 miR164, miR166, miR167, miR168, miR171, miR319, miR390, miR398, miR399,
563 miR408, and miR528 (**Table 1**). The miR390a-3p or miR390b-3p (miR390a/b-3p) of the
564 miR390 family was drought responsive. But no significant regulation on drought was
565 observed for miR390a/b-5p (AAGCUCAGGAGGGAUAGCGCC) that cleaves trans-
566 acting siRNA 3 (TAS3) loci to produce ta-siRNAs (ALLEN *et al.* 2005; WILLIAMS *et al.*
567 2005; DOTTO *et al.* 2014; XIA *et al.* 2017). Predicted TAS3 ta-siRNAs triggered by
568 miR390a/b-5p were either low expressed or with no significant regulation upon drought
569 stress (**Table S10**). For isomiRs, 7, 8, and 3 were in down-regulation, up-regulation, and
570 uncategorized groups, respectively, adding two additional miRNA families, miR396 and
571 miR444, showing drought responses. Notably, multiple isomiRs, and mirR156i-3p, from

572 the miR156 family were up-regulated on drought (**Table 1**). However, miR156j-3p was
573 down-regulated, implying that family members play divergent regulatory roles.
574
575 Targeted protein-coding genes of 21 miRNAs and 18 isomiRs responded to drought were
576 predicted with the psRNATarget tool (DAI AND ZHAO 2011). In total, 67 pairs of gene-
577 miRNA, including 43 non-redundant genes, were predicted to be targeted by 18 drought-
578 responsive miRNAs and isomiRs (**Table S11**). GO enrichment analysis showed that 43
579 miRNA-targeting genes are highly enriched in DNA binding function (GO:0003677, p-
580 value = 2.1E-16) and nucleus cell component (GO:0005634, p-value = 6.1E-16) (**Table**
581 **S12**), suggestive of considerable impacts of miRNAs on the genes regulating
582 transcription under drought stress. Nearly half of targets (18/43) are putative SPL
583 (Squamosa promoter binding protein-like) transcription factors, and 17/18 are targeted by
584 two isomiRs of the miR156 (GACAGAAGAGAGUGAGCACA and
585 UGACAGAAGAGAGUGAGCACA). SPL genes have been reported to be associated
586 with miR156 under drought condition in multiple plant species, such as rice (NIGAM *et al.*
587 2015) cotton (WANG *et al.* 2013), alfalfa (ARSHAD *et al.* 2017), and maize (MAO *et al.*
588 2016). In our result, both SPL-targeting miR156 were up-regulated upon drought (**Figure**
589 **6**), indicating the possible regulation in expression of SPL genes through miRNAs during
590 drought treatment. Another drought-responsive miRNA miR319a/b-3p
591 (UUGGACUGAAGGGUGCUCCC) was predicted to target one MYB and two TCP
592 transcription factors (GRMZM2G028054, GRMZM2G089361, GRMZM2G115516)
593 (ZHANG *et al.* 2009; LIU *et al.* 2014). This miR319a/b-3p remained at a low expression
594 level under high drought stress (**Figure S11**). Presumably, the expression of targeted

595 genes was under a low level of suppression imposed by miR319 under drought condition.
596 Indeed, one of three genes GRMZM2G115516 was up-regulated >4 times on drought
597 (**Table S11**) (LIU *et al.* 2015). The transcriptional regulation of genes targeted by
598 isomiRs of miR156 and miR319a/b-3p was well supported from degradome sequencing
599 data (**Table S11**), which were used to identify miRNA cleavage sites (SHEN *et al.* 2013;
600 ZHAI *et al.* 2013; LIU *et al.* 2014).
601

602 ## Discussion

603 In this study, sRNA sequencing was performed on samples of maize seedlings under
604 drought stress (DS) and well-watered (WW) conditions. The sRNAs were characterized
605 with respect to sRNA lengths, functional class, as well as copy number and epigenetic
606 modifications of sRNA genomic regions. Genomic copy number analysis indicates that
607 most 18-20 nt and 25-30 nt NR-sRNAs and approximately half of the 21-23 nt NR-
608 sRNAs are derived from high-copy genomic repeats. The 24 nt sRNAs were the
609 predominate species among single-copy sRNAs in this study, which is inconsistent with
610 the observations in most other plant species. In fact, 24 nt sRNAs are generally referred
611 to as heterochromatic siRNAs and are primarily derived from intergenic and/or repetitive
612 genomic regions (DUNOYER *et al.* 2007; KASSCHAU *et al.* 2007; AXTELL 2013a).
613 However, 24 nt sRNAs were also recently shown to be enriched in euchromatic regions
614 with low DNA cytosine methylation in an independent maize study (HE *et al.* 2013),
615 which is consistent with our observation. Based on ShortStack sRNA genomic mapping,
616 24-nt sRNA genomic loci were largely located at intergenic regions, but closer to protein-
617 coding genes compared to randomly shuffled simulated loci (**Figure S12**). The proximity

618 of 24-nt sRNA genomic loci to protein-coding genes, particularly highly expressed genes,
619 was previously observed (LUNARDON *et al.* 2016), and the 24-nt sRNA was proposed to
620 function to reinforce silencing of transposable elements close to active genes (LI *et al.*
621 2015a). Our transposon analysis found that 24-nt sRNA genomic loci were over-
622 represented at regions containing DNA transposon elements but under-represented at
623 regions containing LTR retrotransposon elements, *Copia* and *Gypsy* (**Table S13**),
624 suggesting the 24-nt sRNA might be more critical for silencing of DNA transposon
625 elements. Compared to other lengths of sRNAs, genomic regions generating 24 nt sRNAs
626 exhibited low histone modification levels for all histone epimarks examined. Given that
627 most 24 nt sRNAs are generated by PolIV, heavy nucleosome loading and/or strong
628 histone modifications of examined epimarks are likely not prerequisites for transcription
629 via PolIV (LI *et al.* 2015b; LUNARDON *et al.* 2016).
630
631 High proportions of sRNAs with two genomic copies were found in 21 and 22 nt sRNAs
632 but not in 23 or 24 nt sRNAs. Production of most 23 and 24 nt sRNAs requires RNA-
633 dependent RNA polymerase 2 (RDR2) to form dsRNAs and do not require multiple
634 genome copies for optimal function (NOBUTA *et al.* 2008). Two identical copies in the
635 genome could increase the chance for the expression of sense and antisense transcripts to
636 form NAT-siRNAs, which indicates that many 21 and 22 nt sRNAs might be NAT-
637 siRNAs. Genomic regions of 21 and 22 nt sRNAs have the highest modification levels of
638 H3K36me3 among all lengths of sRNAs, resembling H3K36me3 modification levels of
639 internal genic regions (internal exons and introns). The high H3K36me3 signals of 21 and
640 22 nt sRNAs genomic regions are likely contributed by sno-sRNA genomic regions,

641 which exhibited the highest H3K36me3 modification levels. Our results revealed the
642 complexity of histone modifications of plant sRNA genomic regions. However, the lack
643 of high depth of epimark data as well as the different experimental sources between
644 epimark information and sRNA expression data restrict the conclusion about their
645 correlation at a single locus level. Future stratification based on sRNA length, function,
646 as well as genomic and more informative epimark information of sRNA genomic regions
647 would be useful for understanding biogenesis and cellular function as well as further
648 classification of sRNAs.
649
650 Characterization of drought-responsive sRNAs indicates that sRNAs are differentially
651 expressed in response to drought stress. The miRNAs of maize were clustered into three
652 groups based on expression patterns, namely, up-regulated, down-regulated, and
653 transiently down-regulated upon drought stress and over-represented in the down-
654 regulated group, in which miRNAs were approximately 4.8x enriched. The miRNAs and
655 cognate gene targets are involved in drought stress responses in many plant species such
656 as *Arabidopsis* (BUTLER *et al.* 2008), rice (ZHOU *et al.* 2010; FANG *et al.* 2014), soybean
657 (AXTELL 2013b) and poplar (SHUAI *et al.* 2013). Drought-induced miRNAs suppress
658 their target mRNAs, while down-regulated miRNAs result in the de-repression of the
659 target mRNAs (FERDOUS *et al.* 2015). The miRNAs may exhibit distinct responses to
660 drought stress in different plant species (ZHAI *et al.* 2015). For example, miR168a/b
661 down-regulated on drought in rice (ZHOU *et al.* 2010), but was induced in response to
662 drought stress in maize. We have identified 39 drought-responsive miRNAs or isomiRs,
663 as well as their potential gene targets. Detailed studies on their regulatory networks and

664 their functional divergence among species or genotypes within a species would be
665 valuable to modulate miRNA-mediated pathways for improving drought tolerance of
666 plants.
667
668 In addition to miRNAs, sRNAs derived from rRNAs, tRNAs, snoRNAs, and splicing
669 snRNAs were also differentially regulated under drought condition. rRNAs are an
670 essential component of ribosomes and catalyzes protein assembly. rsRNAs (small RNAs
671 derived from rRNAs) were over-represented in the up-regulated sRNA group. rsRNAs
672 were significantly enriched in down-regulated sRNAs after addition of water at 10 DAW.
673 Thus, drought response involves an increase of rsRNAs, which is, in turn, suppressed
674 when water was supplied. Transfer RNAs (tRNAs) play an essential role in protein
675 synthesis. Although tsRNAs (small RNAs derived from tRNAs) are not enriched in either
676 up- or down-regulated sRNAs groups, up-regulated tsRNAs are almost seven times more
677 represented than down-regulated tsRNAs (148/22), which is higher than the ratio of all
678 up-regulated sRNAs to all down-regulated sRNAs (4,373/816). A barley sRNA study
679 also found that tsRNAs, overall, have a tendency to be up-regulated under drought
680 condition (HACKENBERG *et al.* 2015). Both rsRNA and tsRNA were abundant at all
681 lengths from 18 to 27 nt, implying that the cleavage activity of rRNA and tRNA is not
682 size-specific. Likely an unknown RNase III member is involved in rRNA or tRNA
683 cleavage, producing sRNAs with a broad range of lengths (WU *et al.* 2000). Splicing sn-
684 sRNAs, derived from splicing snRNAs that are involved in pre-mRNA splicing, were
685 over-represented in up-regulated sRNAs on drought. Alternative splicing of pre-mRNA
686 splicing under drought stress was observed in multiple tissues, particularly in the leaf and

ear (THATCHER *et al.* 2016), which might partially attributes to amount and stability of various splicing sn-RNAs.

The snoRNAs primarily include two classes of sRNAs, box C/D and box H/ACA snoRNAs, which guide methylation and pseudouridylation of other RNAs, respectively (BACHELLERIE *et al.* 2002; KISS 2006). The snoRNA-mediated chemical modifications of rRNAs and splicing snRNAs have been demonstrated to be essential for ribosomal function as well as mRNA splicing and maturation (MORRIS AND MATTICK 2014; DUPUIS-SANDOVAL *et al.* 2015). The sno-sRNA was over-represented in both down-regulated and transiently down-regulated sRNA groups under drought stress. Down-regulation of sno-sRNAs may be the result of the reduction of snoRNAs, which would reduce the activity of methylation and pseudouridylation of rRNAs and splicing snRNAs. Given the reduction of sno-sRNAs and the increase of rsRNA and splicing sn-sRNAs upon drought stress, it is tempting to speculate that rRNAs and splicing snRNAs are destabilized with decreased methylations or pseudouridylations as mediated by snoRNAs. Both changes in chemical modification, presumably, and the quantity of rRNAs upon drought stress could effectively alter the activity of the protein synthesis machinery. The observation of sRNA changes related to rRNAs and splicing snRNAs indicates the post-transcriptional regulation is an important mechanism for adaptive response to drought stress. snoRNAs exhibiting responses to drought were also found in another plant species (HACKENBERG *et al.* 2015). Recently, snoRNAs were also found to be involved in metabolic stress responses, including oxidative stress in human cells (MICHEL *et al.* 2011; CHU *et al.* 2012; YOUSSEF *et al.* 2015). Taken together, we propose that snoRNAs play a

role to regulate biological processes under drought stress through chemical modifications of rRNAs and splicing snRNAs.

Acknowledgements

This work was supported by the National Key Research and Development Program of China (Grant No. 2016YFD0101002), the National Natural Science Foundation of China (Grant No. 31330056), the Agricultural Science and Technology Innovation Program of CAAS, and the U.S. National Science Foundation (Award No. 1238189). This work of Haiyan Wang was partially supported by a grant from the Simon Foundation (Award# 246077). We thank the support from the Kansas Agricultural Experiment Station (contribution No. 17-132-J).

Authors' contributions

JZ and GW designed the study. JZ, YD, ZJ and KW performed experiments and generated the sequence data. SL, EZ, CH, JF, YH, ML, WL, and HW analyzed data. SL, FW, JZ, and EZ wrote the manuscript. FW, HW, EZ, WL, and GW revised the manuscript. All authors reviewed and approved the final manuscript.

Competing interests

The authors have declared that no conflict of interests exists.

References

Addo-Quaye, C., W. Miller and M. J. Axtell, 2009 CleaveLand: a pipeline for using degradome data to find cleaved small RNA targets. Bioinformatics 25**:** 130-131.

Allen, E., Z. Xie, A. M. Gustafson and J. C. Carrington, 2005 microRNA-directed phasing during trans-acting siRNA biogenesis in plants. Cell 121**:** 207-221.

Arshad, M., B. A. Feyissa, L. Amyot, B. Aung and A. Hannoufa, 2017 MicroRNA156 improves drought stress tolerance in alfalfa (Medicago sativa) by silencing SPL13. Plant Science 258**:** 122-136.

Axtell, M. J., 2013a Classification and comparison of small RNAs from plants. Annual review of plant biology 64**:** 137-159.

Axtell, M. J., 2013b ShortStack: comprehensive annotation and quantification of small RNA genes. RNA 19**:** 740-751.

Bachellerie, J. P., J. Cavaille and A. Huttenhofer, 2002 The expanding snoRNA world. Biochimie 84**:** 775-790.

Benjamini, Y., and Y. Hochberg, 1995 Controlling the false discovery rate - a practical and powerful approach to multiple testing. Journal of the Royal Statistical Society Series B-Methodological 57**:** 289-300.

Burge, S. W., J. Daub, R. Eberhardt, J. Tate, L. Barquist *et al.*, 2013 Rfam 11.0: 10 years of RNA families. Nucleic Acids Res 41**:** D226-232.

Butler, J., I. MacCallum, M. Kleber, I. A. Shlyakhter, M. K. Belmonte *et al.*, 2008 ALLPATHS: de novo assembly of whole-genome shotgun microreads. Genome Res 18**:** 810-820.

Chantalat, S., A. Depaux, P. Hery, S. Barral, J. Y. Thuret *et al.*, 2011 Histone H3 trimethylation at lysine 36 is associated with constitutive and facultative heterochromatin. Genome Res 21**:** 1426-1437.

Chu, L., M. Y. Su, L. B. Maggi, Jr., L. Lu, C. Mullins *et al.*, 2012 Multiple myeloma-associated chromosomal translocation activates orphan snoRNA ACA11 to suppress oxidative stress. J Clin Invest 122**:** 2793-2806.

Covarrubias, A. A., and J. L. Reyes, 2010 Post-transcriptional gene regulation of salinity and drought responses by plant microRNAs. Plant Cell Environ 33**:** 481-489.

Dai, X., and P. X. Zhao, 2011 psRNATarget: a plant small RNA target analysis server. Nucleic Acids Res 39**:** W155-159.

Ding, Y., Y. Tao and C. Zhu, 2013 Emerging roles of microRNAs in the mediation of drought stress response in plants. J Exp Bot 64**:** 3077-3086.

Dotto, M. C., K. A. Petsch, M. J. Aukerman, M. Beatty, M. Hammell *et al.*, 2014 Genome-wide analysis of leafbladeless1-regulated and phased small RNAs underscores the importance of the TAS3 ta-siRNA pathway to maize development. Plos Genet 10.

Dunoyer, P., C. Himber, V. Ruiz-Ferrer, A. Alioua and O. Voinnet, 2007 Intra- and intercellular RNA interference in Arabidopsis thaliana requires components of the microRNA and heterochromatic silencing pathways. Nat Genet 39**:** 848-856.

Dupuis-Sandoval, F., M. Poirier and M. S. Scott, 2015 The emerging landscape of small nucleolar RNAs in cell biology. Wiley Interdiscip Rev RNA 6**:** 381-397.

Fang, Y., K. Xie and L. Xiong, 2014 Conserved miR164-targeted NAC genes negatively regulate drought resistance in rice. J Exp Bot 65**:** 2119-2135.

Ferdous, J., S. S. Hussain and B. J. Shi, 2015 Role of microRNAs in plant drought tolerance. Plant Biotechnol J 13**:** 293-305.

Fraley, C., and A. E. Raftery, 2007 Model-based methods of classification: Using the mclust software in chemometrics. J Stat Softw 18.

780 Gan, E. S., Y. Xu and T. Ito, 2015 Dynamics of H3K27me3 methylation and
781 demethylation in plant development. Plant Signal Behav 10**:** e1027851.
782 Hackenberg, M., P. Gustafson, P. Langridge and B. J. Shi, 2015 Differential expression
783 of microRNAs and other small RNAs in barley between water and drought
784 conditions. Plant Biotechnol J 13**:** 2-13.
785 He, G., B. Chen, X. Wang, X. Li, J. Li *et al.*, 2013 Conservation and divergence of
786 transcriptomic and epigenomic variation in maize hybrids. Genome Biol 14**:** R57.
787 Kasschau, K. D., N. Fahlgren, E. J. Chapman, C. M. Sullivan, J. S. Cumbie *et al.*, 2007
788 Genome-wide profiling and analysis of Arabidopsis siRNAs. PLoS biology 5**:**
789 e57.
790 Khraiwesh, B., J.-K. Zhu and J. Zhu, 2012 Role of miRNAs and siRNAs in biotic and
791 abiotic stress responses of plants. Biochimica et Biophysica Acta (BBA) - Gene
792 Regulatory Mechanisms 1819**:** 137-148.
793 Kiss, T., 2006 SnoRNP biogenesis meets Pre-mRNA splicing. Mol Cell 23**:** 775-776.
794 Kozomara, A., and S. Griffiths-Jones, 2014 miRBase: annotating high confidence
795 microRNAs using deep sequencing data. Nucleic Acids Res 42**:** D68-73.
796 Langfelder, P., and S. Horvath, 2008 WGCNA: an R package for weighted correlation
797 network analysis. BMC Bioinformatics 9**:** 559.
798 Li, H., and R. Durbin, 2010 Fast and accurate long-read alignment with Burrows-
799 Wheeler transform. Bioinformatics 26**:** 589-595.
800 Li, J. S., F. L. Fu, M. An, S. F. Zhou, Y. H. She *et al.*, 2013 Differential Expression of
801 MicroRNAs in Response to Drought Stress in Maize. Journal of Integrative
802 Agriculture 12**:** 1414-1422.
803 Li, Q., J. I. Gent, G. Zynda, J. W. Song, I. Makarevitch *et al.*, 2015a RNA-directed DNA
804 methylation enforces boundaries between heterochromatin and euchromatin in the
805 maize genome. Proceedings of the National Academy of Sciences of the United
806 States of America 112**:** 14728-14733.
807 Li, S. F., L. E. Vandivier, B. Tu, L. Gao, S. Y. Won *et al.*, 2015b Detection of Pol
808 IV/RDR2-dependent transcripts at the genomic scale in Arabidopsis reveals
809 features and regulation of siRNA biogenesis. Genome Research 25**:** 235-245.
810 Liang, H., and L. F. Landweber, 2007 Hypothesis: RNA editing of microRNA target sites
811 in humans? RNA 13**:** 463-467.
812 Liu, H., C. Qin, Z. Chen, T. Zuo, X. Yang *et al.*, 2014 Identification of miRNAs and their
813 target genes in developing maize ears by combined small RNA and degradome
814 sequencing. BMC Genomics 15**:** 25.
815 Liu, Y., M. Zhou, Z. Gao, W. Ren, F. Yang *et al.*, 2015 RNA-Seq analysis reveals
816 MAPKKK family members related to drought tolerance in maize. PLoS One 10**:**
817 e0143128.
818 Love, M. I., W. Huber and S. Anders, 2014 Moderated estimation of fold change and
819 dispersion for RNA-seq data with DESeq2. Genome Biol 15**:** 550.
820 Lunardon, A., C. Forestan, S. Farinati, M. J. Axtell and S. Varotto, 2016 Genome-Wide
821 Characterization of Maize Small RNA Loci and Their Regulation in the required
822 to maintain repression6-1 (rmr6-1) Mutant and Long-Term Abiotic Stresses. Plant
823 Physiol 170**:** 1535-1548.

824 Mao, H., L. Yu, Z. Li, Y. Yan, R. Han *et al.*, 2016 Genome-wide analysis of the SPL
825 family transcription factors and their responses to abiotic stresses in maize. Plant
826 Gene 6**:** 1-12.
827 Marcais, G., and C. Kingsford, 2011 A fast, lock-free approach for efficient parallel
828 counting of occurrences of k-mers. Bioinformatics 27**:** 764-770.
829 Meyers, B. C., M. Matzke and V. Sundaresan, 2008 The RNA world is alive and well.
830 Trends in Plant Science 13**:** 311-313.
831 Michel, C. I., C. L. Holley, B. S. Scruggs, R. Sidhu, R. T. Brookheart *et al.*, 2011 Small
832 nucleolar RNAs U32a, U33, and U35a are critical mediators of metabolic stress.
833 Cell Metab 14**:** 33-44.
834 Morin, R. D., M. D. O'Connor, M. Griffith, F. Kuchenbauer, A. Delaney *et al.*, 2008
835 Application of massively parallel sequencing to microRNA profiling and
836 discovery in human embryonic stem cells. Genome Res 18**:** 610-621.
837 Morris, K. V., and J. S. Mattick, 2014 The rise of regulatory RNA. Nat Rev Genet 15**:**
838 423-437.
839 Nigam, D., S. Kumar, D. C. Mishra, A. Rai, S. Smita *et al.*, 2015 Synergistic regulatory
840 networks mediated by microRNAs and transcription factors under drought, heat
841 and salt stresses in Oryza Sativa spp. Gene 555**:** 127-139.
842 Nobuta, K., C. Lu, R. Shrivastava, M. Pillay, E. De Paoli *et al.*, 2008 Distinct size
843 distribution of endogeneous siRNAs in maize: Evidence from deep sequencing in
844 the mop1-1 mutant. Proc Natl Acad Sci U S A 105**:** 14958-14963.
845 Onodera, Y., J. R. Haag, T. Ream, P. Costa Nunes, O. Pontes *et al.*, 2005 Plant nuclear
846 RNA polymerase IV mediates siRNA and DNA methylation-dependent
847 heterochromatin formation. Cell 120**:** 613-622.
848 Rhoades, M. W., B. J. Reinhart, L. P. Lim, C. B. Burge, B. Bartel *et al.*, 2002 Prediction
849 of plant microRNA targets. Cell 110**:** 513-520.
850 Schnable, P. S., D. Ware, R. S. Fulton, J. C. Stein, F. Wei *et al.*, 2009 The B73 maize
851 genome: complexity, diversity, and dynamics. Science 326**:** 1112-1115.
852 Shen, Y., Z. Jiang, S. Lu, H. Lin, S. Gao *et al.*, 2013 Combined small RNA and
853 degradome sequencing reveals microRNA regulation during immature maize
854 embryo dedifferentiation. Biochem Biophys Res Commun 441**:** 425-430.
855 Shuai, P., D. Liang, Z. Zhang, W. Yin and X. Xia, 2013 Identification of drought-
856 responsive and novel Populus trichocarpa microRNAs by high-throughput
857 sequencing and their targets using degradome analysis. BMC Genomics 14**:** 233.
858 Stroud, H., M. V. Greenberg, S. Feng, Y. V. Bernatavichute and S. E. Jacobsen, 2013
859 Comprehensive analysis of silencing mutants reveals complex regulation of the
860 Arabidopsis methylome. Cell 152**:** 352-364.
861 Thatcher, S. R., O. N. Danilevskaya, X. Meng, M. Beatty, G. Zastrow-Hayes *et al.*, 2016
862 Genome-wide analysis of alternative splicing during development and drought
863 stress in maize. Plant Physiol 170**:** 586-599.
864 Tian, T., Y. Liu, H. Yan, Q. You, X. Yi *et al.*, 2017 agriGO v2.0: a GO analysis toolkit
865 for the agricultural community, 2017 update. Nucleic Acids Res 45**:** W122-W129.
866 Vazquez, F., S. Legrand and D. Windels, 2010 The biosynthetic pathways and biological
867 scopes of plant small RNAs. Trends in Plant Science 15**:** 337-345.
868 Wang, M., Q. L. Wang and B. H. Zhang, 2013 Response of miRNAs and their targets to
869 salt and drought stresses in cotton (Gossypium hirsutum L.). Gene 530**:** 26-32.

870 Wang, X., A. A. Elling, X. Li, N. Li, Z. Peng *et al.*, 2009 Genome-wide and organ-
871 specific landscapes of epigenetic modifications and their relationships to mRNA
872 and small RNA transcriptomes in maize. Plant Cell 21**:** 1053-1069.
873 Wang, Y. G., M. An, S. F. Zhou, Y. H. She, W. C. Li *et al.*, 2014 Expression profile of
874 maize microRNAs corresponding to their target genes under drought stress.
875 Biochemical Genetics 52**:** 474-493.
876 West, P. T., Q. Li, L. Ji, S. R. Eichten, J. Song *et al.*, 2014 Genomic distribution of
877 H3K9me2 and DNA methylation in a maize genome. PLoS One 9**:** e105267.
878 Wierzbicki, A. T., J. R. Haag and C. S. Pikaard, 2008 Noncoding transcription by RNA
879 polymerase Pol IVb/Pol V mediates transcriptional silencing of overlapping and
880 adjacent genes. Cell 135**:** 635-648.
881 Williams, L., C. C. Carles, K. S. Osmont and J. C. Fletcher, 2005 A database analysis
882 method identifies an endogenous trans-acting short-interfering RNA that targets
883 the Arabidopsis ARF2, ARF3, and ARF4 genes. Proc Natl Acad Sci U S A 102**:**
884 9703-9708.
885 Wu, H., H. Xu, L. J. Miraglia and S. T. Crooke, 2000 Human RNase III is a 160-kDa
886 protein involved in preribosomal RNA processing. J Biol Chem 275**:** 36957-
887 36965.
888 Xia, R., J. Xu and B. C. Meyers, 2017 The Emergence, Evolution, and Diversification of
889 the miR390-TAS3-ARF Pathway in Land Plants. Plant Cell 29**:** 1232-1247.
890 Young, M. D., M. J. Wakefield, G. K. Smyth and A. Oshlack, 2010 Gene ontology
891 analysis for RNA-seq: accounting for selection bias. Genome Biol 11**:** R14.
892 Youssef, O. A., S. A. Safran, T. Nakamura, D. A. Nix, G. S. Hotamisligil *et al.*, 2015
893 Potential role for snoRNAs in PKR activation during metabolic stress. Proc Natl
894 Acad Sci U S A 112**:** 5023-5028.
895 Zhai, J., H. Zhang, S. Arikit, K. Huang, G.-L. Nan *et al.*, 2015 Spatiotemporally dynamic,
896 cell-type–dependent premeiotic and meiotic phasiRNAs in maize anthers.
897 Proceedings of the National Academy of Sciences 112**:** 201418918.
898 Zhai, L., Z. Liu, X. Zou, Y. Jiang, F. Qiu *et al.*, 2013 Genome-wide identification and
899 analysis of microRNA responding to long-term waterlogging in crown roots of
900 maize seedlings. Physiol Plant 147**:** 181-193.
901 Zhang, B., 2015 MicroRNA: a new target for improving plant tolerance to abiotic stress.
902 J Exp Bot 66**:** 1749-1761.
903 Zhang, L., J. M. Chia, S. Kumari, J. C. Stein, Z. Liu *et al.*, 2009 A genome-wide
904 characterization of microRNA genes in maize. PLoS Genet 5**:** e1000716.
905 Zheng, J., J. J. Fu, M. Y. Gou, J. L. Huai, Y. J. Liu *et al.*, 2010 Genome-wide
906 transcriptome analysis of two maize inbred lines under drought stress. Plant
907 Molecular Biology 72**:** 407-421.
908 Zhou, L., Y. Liu, Z. Liu, D. Kong, M. Duan *et al.*, 2010 Genome-wide identification and
909 analysis of drought-responsive microRNAs in Oryza sativa. J Exp Bot 61**:** 4157-
910 4168.
911 Zhu, J. K., 2002 Salt and drought stress signal transduction in plants. Annu Rev Plant
912 Biol 53**:** 247-273.
913

914

915 **Table 1**. The list of drought-responsive miRNAs

miRNA sequence	Len (nt)	Total reads[1]	Genomic copy[2]	miRNA gene	miRNA type	Cluster group[3]
UGGGUGUCAUCUCGCCUGAAGC	22	531	1	MIR1432	3p	Others
UCAGGAGAGAUGACACCGACG	21	9,059	1	MIR1432	5p	UP
GACAGAAGAGAGUGAGCACA	20	9,921	8	MIR156a,b,c,d,e,h,i,l, Cluster_27697	isomiR	UP
UGACAGAAGAGAGUGAGCACA	21	23,675	8	MIR156a,b,c,d,e,h,i,l, Cluster_27697	isomiR	UP
ACGGCGCGACGAACGACAUAGC	22	1,417	1	MIR156d	isomiR	Others
GCUCACUGCUCUAUCUGUCAUC	22	14,829	1	MIR156i	3p	UP
GCUCACUGCUCUAUCUGUCAU	21	1,116	1	MIR156i	isomiR	UP
GCUCUCUGCUCUCACUGUCAUC	22	607	1	MIR156j	3p	DOWN
CACGUGCUCCCCUUCUCCACC	21	499	1	MIR164g	3p	DOWN
GGAAUGUUGUCUGGUUCAAGG	21	40,096	2	MIR166b,d	5p	DOWN
GGAAUGUUGUCUGGUUCAAGGU	22	839	4	MIR166b,d	isomiR	DOWN
GGAAUGUCGUCUGGCGCGAGA	21	416	1	MIR166i	5p	DOWN
GGUUUGUUUGUCUGGUUCAAGG	22	2,613	1	MIR166j	5p	DOWN
GGAAUGUUGGCUGGCUCGAGG	21	2,563	2	MIR166m, Cluster_45700	5p	DOWN
GAUCAUGCUGUGGCAGCCUCACU	23	3,287	1	MIR167c	3p	DOWN
AGGUCAUGCUGUAGUUUCAUC	21	3,986	1	MIR167g	isomiR	DOWN
AGAUCAUGUGGCAGUUUCAUU	21	2,807	1	MIR167j	isomiR	UP
CCCGCCUUGCACCAAGUGAA	20	25,019	1	MIR168a	3p	UP
CGCUUGGUGCAGAUCGGGAC	20	19,995	2	MIR168a,b	isomiR	UP
UCGCUUGGUGCAGAUCGGGA	20	294,017	2	MIR168a,b	isomiR	UP
UCGCUUGGUGCAGAUCGGGACC	22	59,451	2	MIR168a,b	isomiR	UP
UGUUGGCUCGGCUCACUCAGA	21	21,299	2	MIR171d,e	5p	DOWN
UUGGACUGAAGGGUGCUCCC	20	62,868	4	MIR319a,b,c,d	3p	Others
CGCUAUCUAUCCUGAGCUCCA	21	9,684	2	MIR390a,b	3p	DOWN
CAGCUUUCUUGAACUUCUUCU	21	823	2	MIR396e,f	isomiR	DOWN
GGGGCGAACUGAGAACACAUG	21	5,992	1	MIR398a	5p	DOWN
AUGUGUUCUCAGGUCGCCCCCG	22	1,920	2	MIR398a,b	isomiR	Others
GGGGCGGACUGGGAACACAUG	21	53,148	1	MIR398b	5p	DOWN
GGGCGGACUGGGAACACAUGG	21	10,086	1	MIR398b	isomiR	DOWN
GGGUACGUCUCCUUUGGCACA	21	390	1	MIR399c	5p	Others
GGGCUUCUCUUUCUUGGCAGG	21	2,098	1	MIR399e	5p	Others
GGGCAACUUCUCCUUUGGCAGA	22	2,743	1	MIR399f	5p	UP
CAGGGAUGAGACAGAGCAUG	20	12,523	1	MIR408a	isomiR	DOWN
CAGGGAUGAGACAGAGCAUGG	21	51,773	1	MIR408a	isomiR	DOWN
CAGGGACGAGGCAGAGCAUGG	21	6,822	1	MIR408b	5p	DOWN
CAGGGACGAGGCAGAGCAUG	20	10,218	1	MIR408b	isomiR	Others
UGCAAGUUGUGCAGUUGUUGU	21	2,125	3	MIR444a,b	isomiR	UP
CCUGUGCCUGCCUCUUCCAUU	21	8,186	2	MIR528a,b	3p	DOWN
CUGUGCCUGCCUCUUCCAUU	20	1,137	2	MIR528a,b	isomiR	DOWN

916 [1] total sRNA reads from all 36 samples
917 [2] Genomic DNA copy number using the reference-based method
918 [3] Clustering group from the mclust analysis. Down and Up represent down-regulated and up-
919 regulated groups respectively on drought stress. Others represent the group that does not belong
920 to down-regulated, up-regulated, or transiently down regulated groups.
921

Figure legends

Figure 1. Morphological and physiological changes of maize seedlings during drought stress. (A) Three-day-old B73 seedlings were subjected to gradual drought stress or well-watered conditions. The photos were taken at each day from 3 to 11 days. Bar=5cm. (B) The changing curves of water content of soil (SWC) from five replicated pots of each data point. (C) Leaf relative water content (RWC) of seedlings along days. (D) Leaf relative electrical conductivity (REC) of seedlings along days. Red and green curves represent plants under drought stress and well water, respectively. Five seedlings were pooled as one replicate, and five independent biological replicates were conducted to determine RWC and REC. Vertical lines represent standard errors.

Figure 2. Characterization of sRNAs. (A) Proportions of sRNAs of different lengths in all samples. Each curve represents a sample. WW, DS, and DWR, represent well-watered, drought stress, and drought water recovered plants, respectively. (B-D) Overview of genomic copy number, lengths, functional categories, and expression of NR-sRNAs from all the samples. (B) Pie chart of distribution of different classes of sRNAs. Others represent sRNAs that were not unambiguously categorized. (C) Stacked barplot of different functional classes of NR-sRNAs at varying sizes of sRNAs from 18 to 30 nt. (D) Stacked barplot of different functional classes of sRNA reads, representing expression levels, at varying lengths of sRNAs from 18 to 30 nt. (E) Density plots of expression levels of different functional classes of sRNAs. Density on the y-axis represents the probability of sRNA occurrences. (F) Density plots of expression levels of different lengths of sRNAs. Density on the y-axis represents the probability of sRNA occurrences.

945

946 **Figure 3**. Modification levels of five epimarks on sRNA genomic regions. The average
947 ChIP-Seq signals, represented by read depths of ChIP-Seq, of five epimarks were
948 determined and normalized by sequencing library sizes separately. Heights of bars
949 represent relative histone modification levels. The general function of each epimark is
950 briefly described in the subtitle of each barplot.

951

952 **Figure 4**. Major clusters of drought-responsive sRNAs. Drought-responsive sRNAs were
953 subjected to clustering using the software mclust, which ended with 10 clusters. Nine
954 major clusters (A-E, G, H, J, K) were classified into three groups, up-regulated (light
955 blue), down-regulated (light orange), and transiently down-regulated (light purple). Each
956 curve represents an average sRNA expression ratio of drought stress to well-watered with
957 a Log2 transformation from two biological replicates along DAW. Three pie charts
958 designate proportions of different classes of sRNAs that were functionally annotated in
959 each of the three clustering groups: up-regulated (F); down-regulated (I); transiently
960 down-regulated (L).

961

962 **Figure 5**. sRNA co-expression networks
963 (A) Visualization of the DS network using Cytoscape, each node represents an sRNA and
964 each line is the edge connecting sRNA nodes. Five modules (sub-network) were
965 highlighted by different colors. (B) Visualization of the WW network. Six modules (sub-
966 networks) were highlighted by different colors. Note that assignment of colors in (A) and
967 (B) are sort of independent. The same color might not represent the same group of

968 sRNAs. (C) Result of the module preservation analysis performed to evaluate whether a
969 module identified in the DS network is preserved in the WW network. The color code
970 corresponds to that used in (A). (D) Result of the module preservation analysis of the
971 WW network in comparison with the WW network. The color code corresponds to that
972 used in (B).
973
974 **Figure 6**. Time-series expression profiles of two miR156 targeting SPL genes
975 (A, B) Normalized counts of each miR156 (y-axis) were plotted along 3-11 DAW. WW,
976 DS, DWR represent well-watered, drought stress, drought water recovery, respectively. A
977 sequence on the top of each plot is the miR156 sequence. Each error bar represents the
978 range of a standard error above and below each mean value.
979

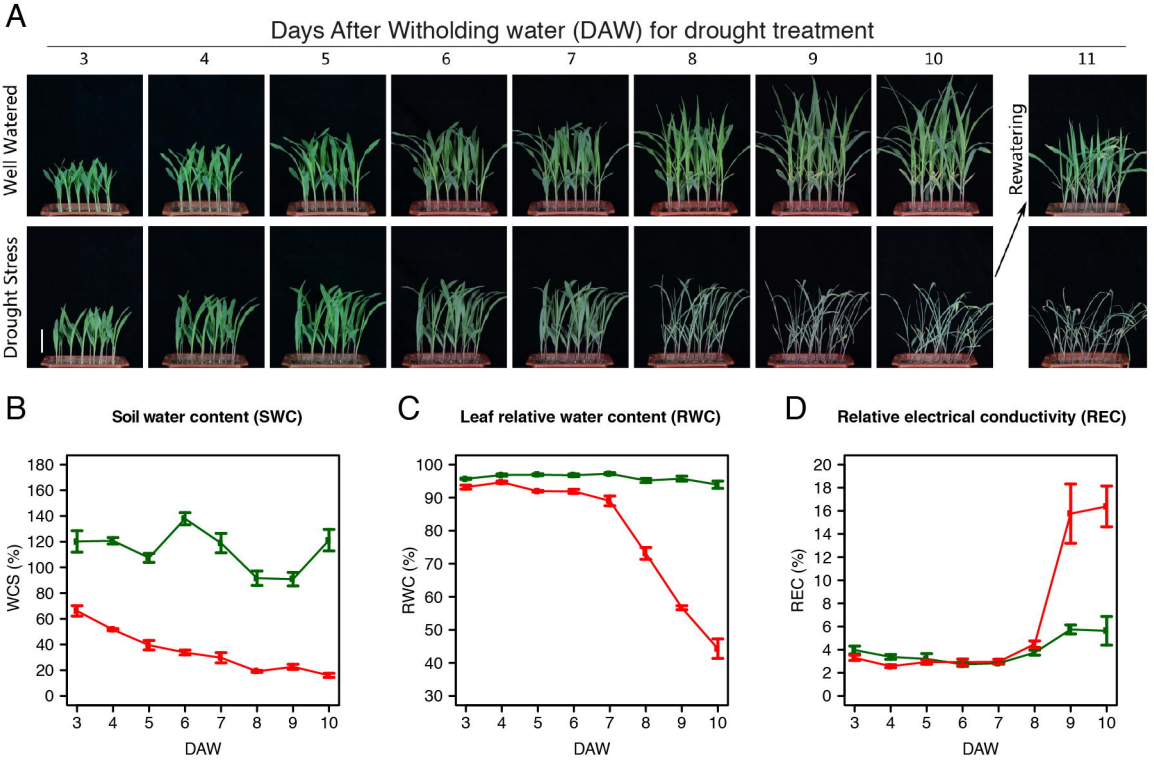
A
Days After Witholding water (DAW) for drought treatment
3
4
5
6
7
8
9
10
11
Well Watered
Drought Stress
Rewatering
B
Soil water content (SWC)
WCS (%)
DAW
C
Leaf relative water content (RWC)
RWC (%)
DAW
D
Relative electrical conductivity (REC)
REC (%)
DAW

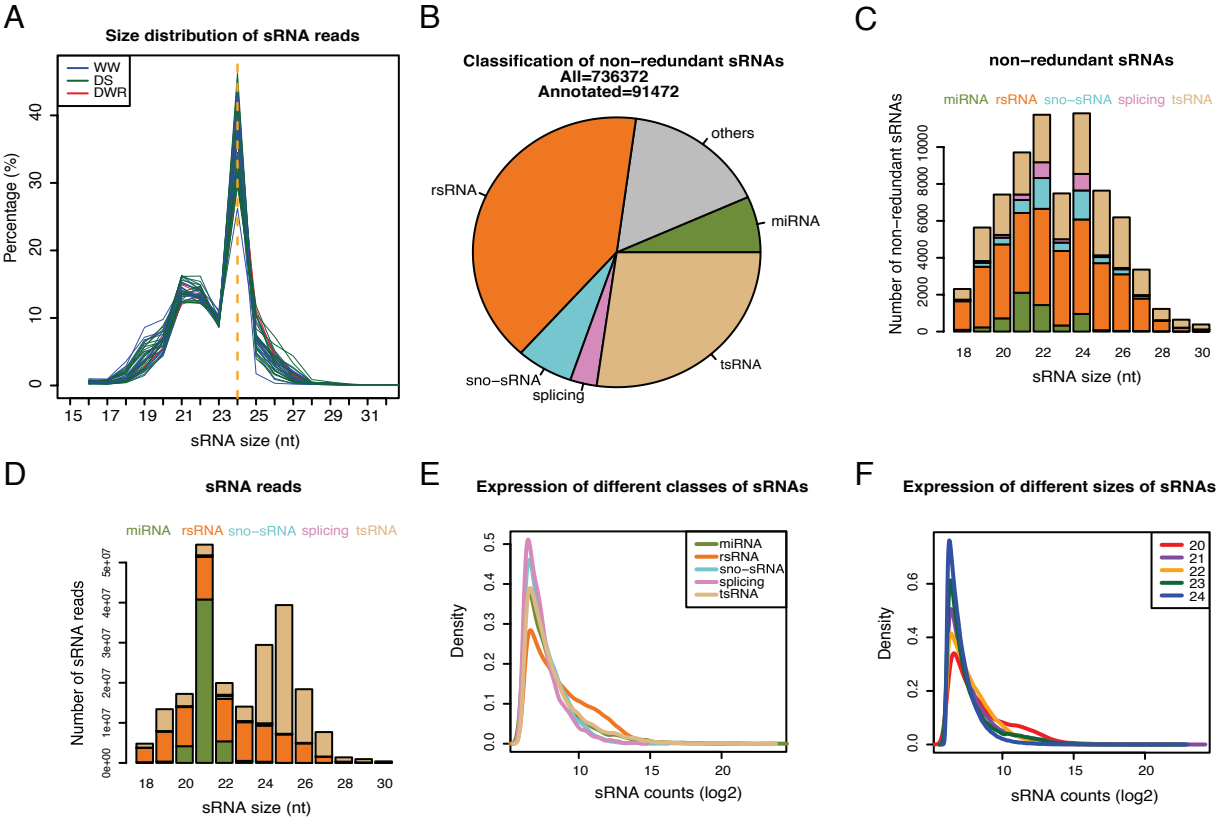
A
Size distribution of sRNA reads
WW
DS
DWR
Percentage (%)
sRNA size (nt)
B
Classification of non−redundant sRNAs
All=736372
Annotated=91472
others
miRNA
tsRNA
splicing
sno−sRNA
rsRNA
C
non−redundant sRNAs
miRNA rsRNA sno−sRNA splicing tsRNA
Number of non−redundant sRNAs
sRNA size (nt)
D
sRNA reads
miRNA rsRNA sno−sRNA splicing tsRNA
Number of sRNA reads
sRNA size (nt)
E
Expression of different classes of sRNAs
miRNA
rsRNA
sno−sRNA
splicing
tsRNA
Density
sRNA counts (log2)
F
Expression of different sizes of sRNAs
20
21
22
23
24
Density
sRNA counts (log2)

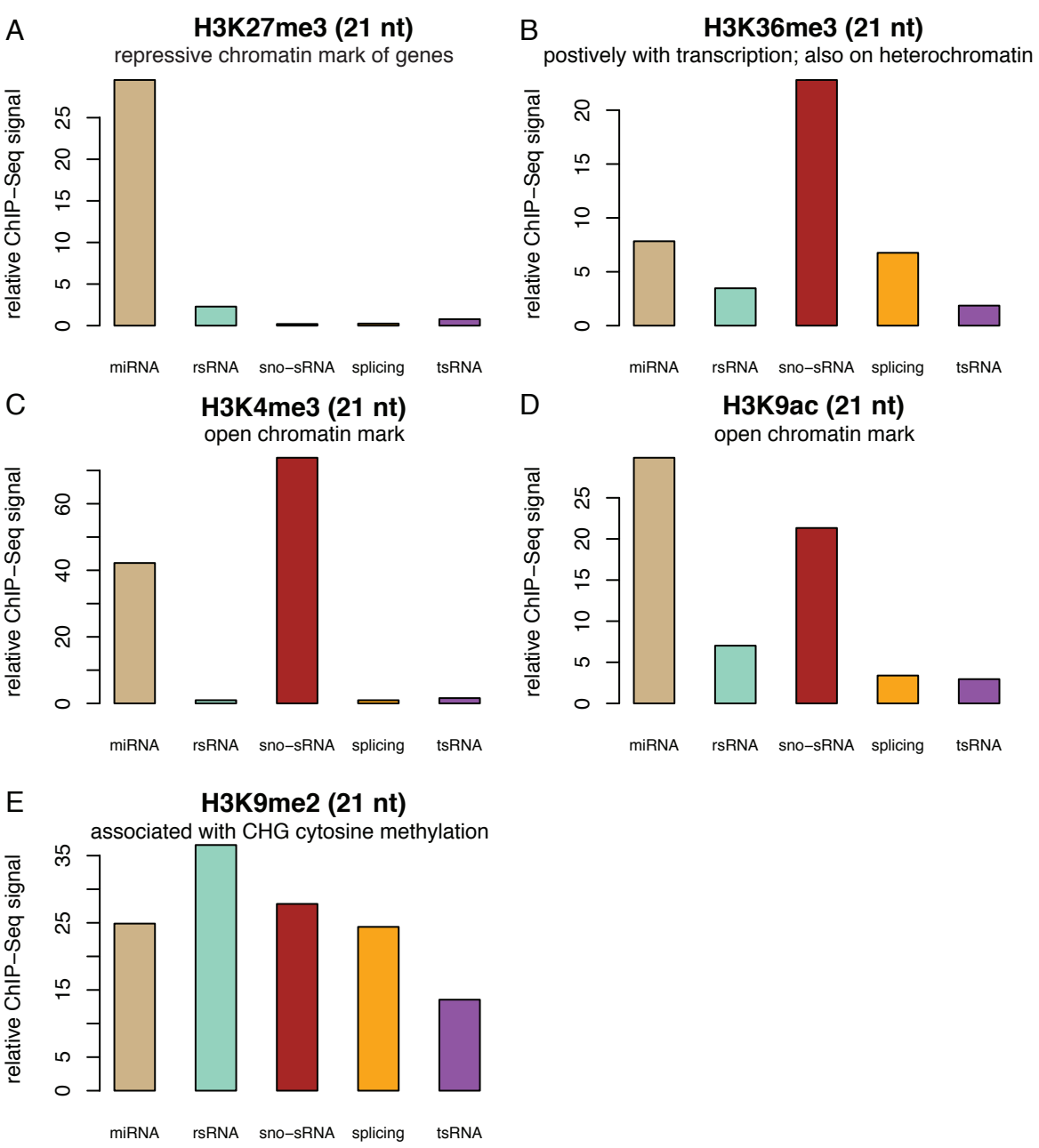
A
H3K27me3 (21 nt)
repressive chromatin mark of genes
relative ChIP−Seq signal
0
5
10
15
20
25
miRNA
rsRNA
sno−sRNA
splicing
tsRNA
B
H3K36me3 (21 nt)
postively with transcription; also on heterochromatin
relative ChIP−Seq signal
0
5
10
15
20
miRNA
rsRNA
sno−sRNA
splicing
tsRNA
C
H3K4me3 (21 nt)
open chromatin mark
relative ChIP−Seq signal
0
20
40
60
miRNA
rsRNA
sno−sRNA
splicing
tsRNA
D
H3K9ac (21 nt)
open chromatin mark
relative ChIP−Seq signal
0
5
10
15
20
25
miRNA
rsRNA
sno−sRNA
splicing
tsRNA
E
H3K9me2 (21 nt)
associated with CHG cytosine methylation
relative ChIP−Seq signal
0
5
15
25
35
miRNA
rsRNA
sno−sRNA
splicing
tsRNA

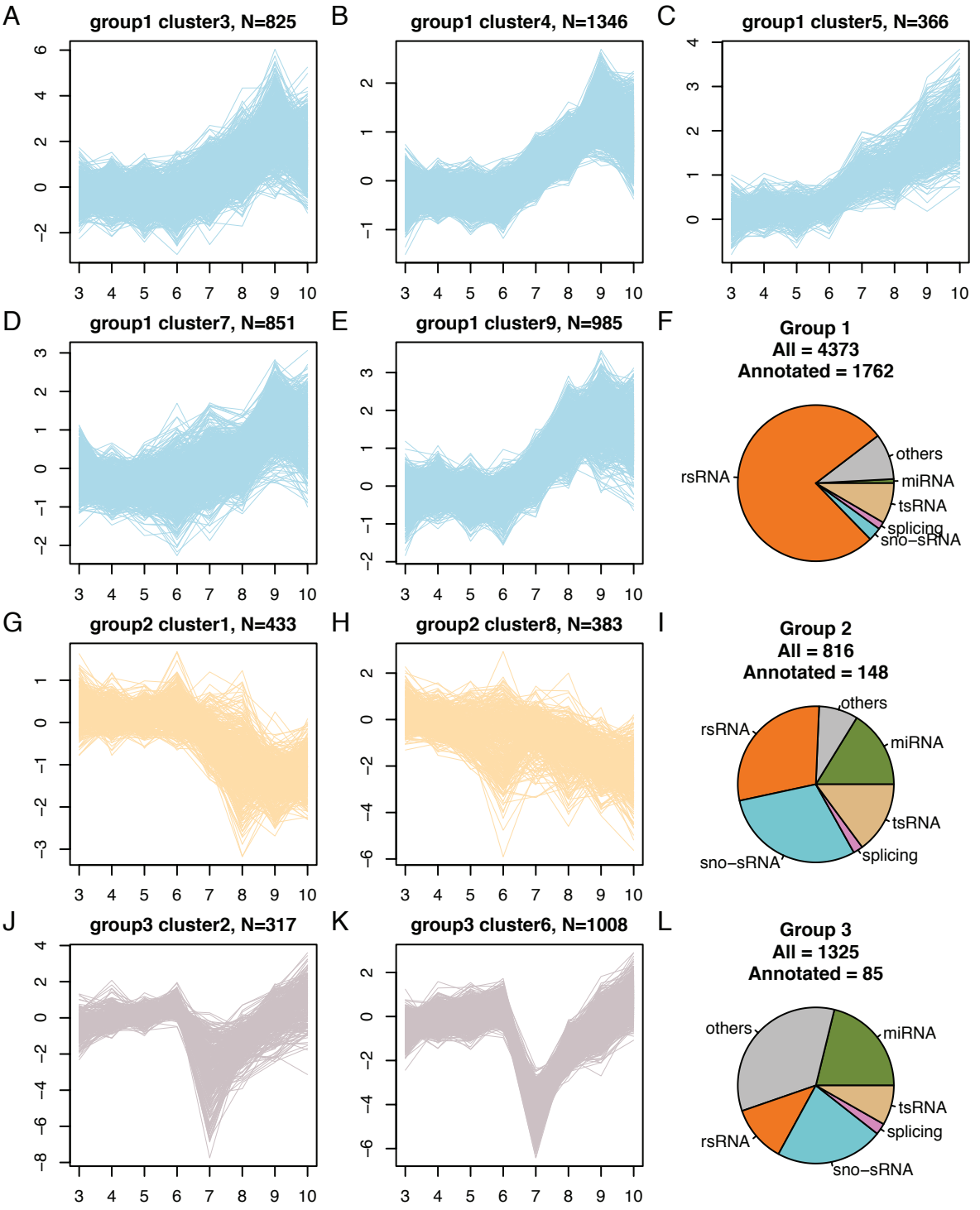
A
group1 cluster3, N=825
B
group1 cluster4, N=1346
C
group1 cluster5, N=366
D
group1 cluster7, N=851
E
group1 cluster9, N=985
F
Group 1
All = 4373
Annotated = 1762
rsRNA
others
miRNA
tsRNA
splicing
sno−sRNA
G
group2 cluster1, N=433
H
group2 cluster8, N=383
I
Group 2
All = 816
Annotated = 148
rsRNA
others
miRNA
tsRNA
splicing
sno−sRNA
J
group3 cluster2, N=317
K
group3 cluster6, N=1008
L
Group 3
All = 1325
Annotated = 85
others
miRNA
tsRNA
splicing
rsRNA
sno−sRNA

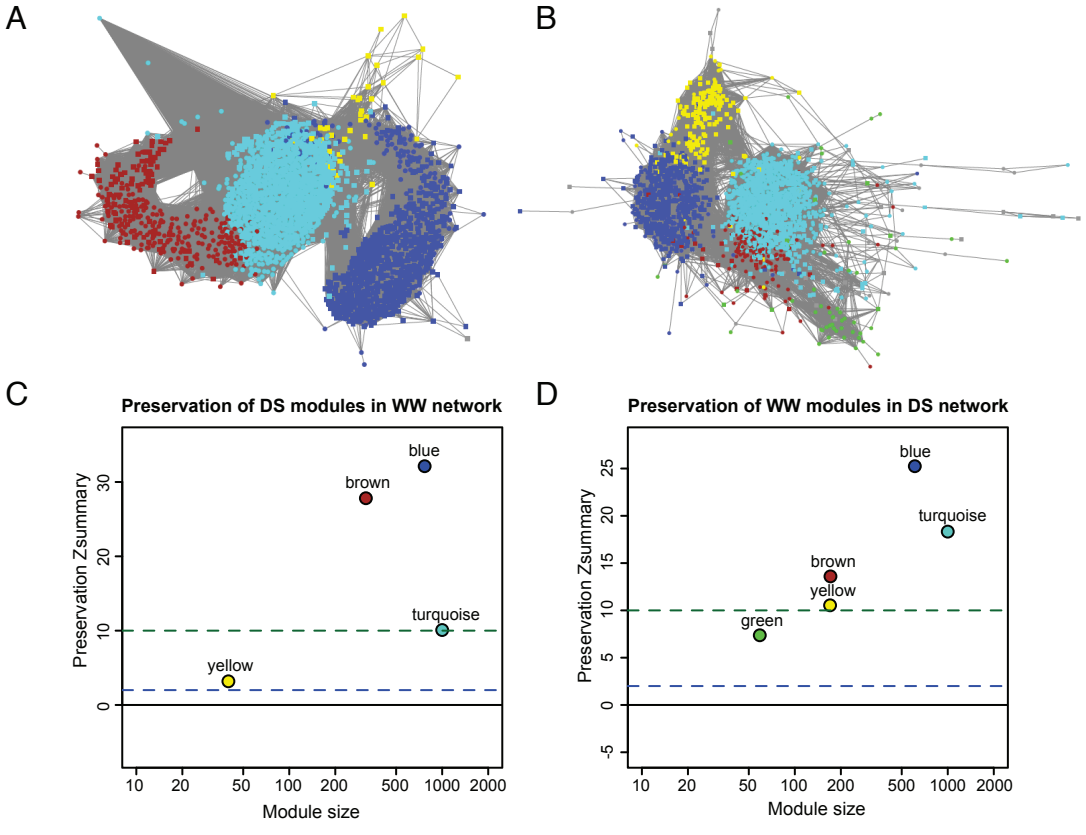
A
B
C
Preservation of DS modules in WW network
blue
brown
turquoise
yellow
Preservation Zsummary
Module size
10
20
50
100
200
500
1000
2000
0
10
20
30
D
Preservation of WW modules in DS network
blue
turquoise
brown
yellow
green
Preservation Zsummary
Module size
-5
0
5
10
15
20
25

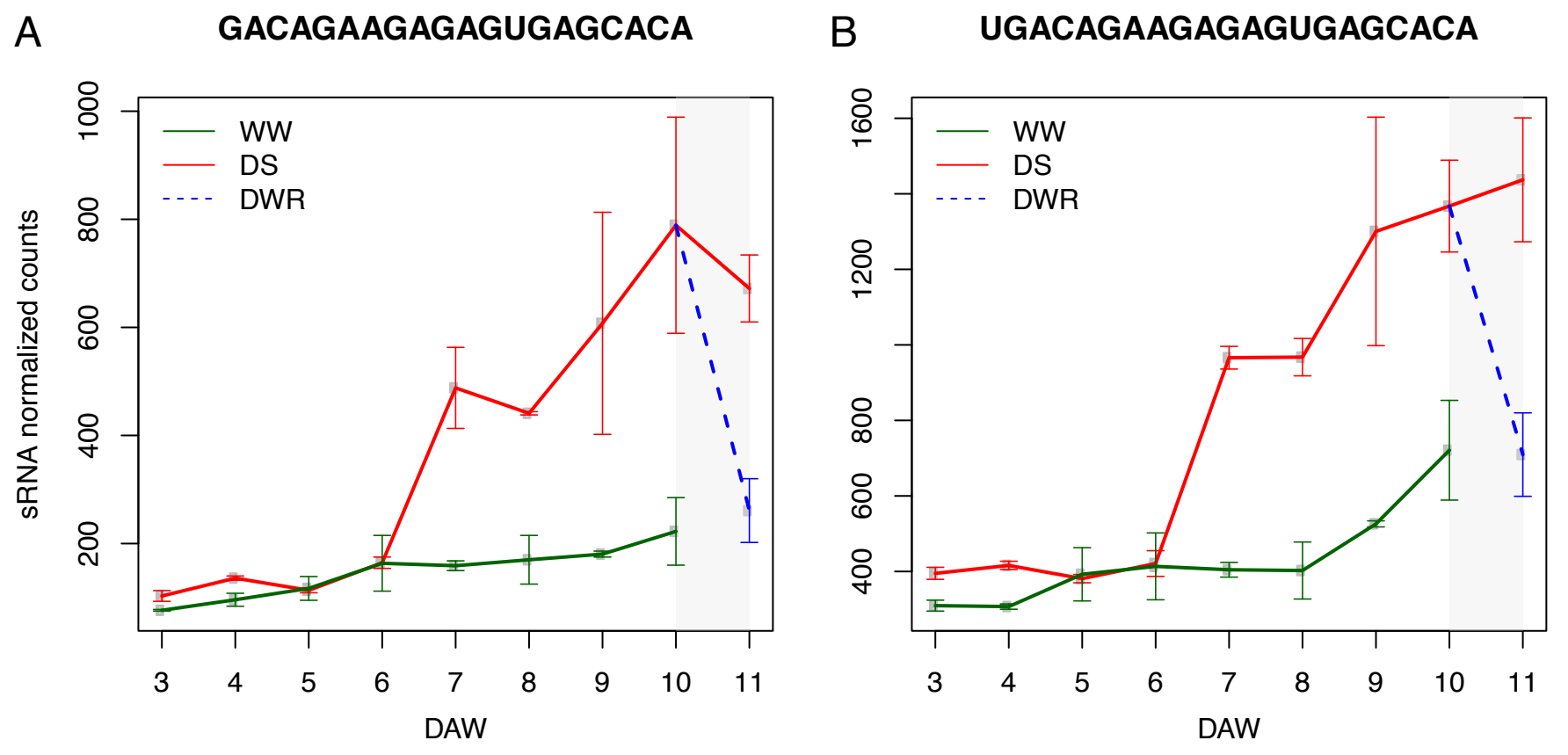
A
GACAGAAGAGAGUGAGCACA
sRNA normalized counts
200
400
600
800
1000
WW
DS
DWR
3
4
5
6
7
8
9
10
11
DAW
B
UGACAGAAGAGAGUGAGCACA
400
600
800
1200
1600
WW
DS
DWR
3
4
5
6
7
8
9
10
11
DAW